WRF-Simulated Low-Level Jets over Iowa: Characterization and Sensitivity Studies

Jeanie A. Aird[1], Rebecca J. Barthelmie[1], Tristan J. Shepherd[2], Sara C. Pryor[2]

[1]Sibley School of Mechanical and Aerospace Engineering, Cornell University, Ithaca, New York, USA
5   [2]Department of Earth and Atmospheric Sciences, Cornell University, Ithaca, New York, USA

Correspondence to: J. A. Aird (jaa377@cornell.edu)

Abstract. Output from high resolution simulations with the Weather Research and Forecasting (WRF) model are analyzed to characterize local low level jets (LLJ) over Iowa. Analyses using a detection algorithm wherein the wind speed above and below the jet maximum must be below 80% of the jet wind speed within a vertical window

10   of approximately 20 m – 530 m a.g.l. indicate the presence of a LLJ in at least one of the 14700 4 km by 4 km grid cells over Iowa on 98% of nights. Nocturnal LLJ are most frequently associated with stable stratification and low TKE and hence are more frequent during the winter months. The spatiotemporal mean LLJ maximum (jet core) wind speed is 9.55 ms⁻¹ and the mean height is 182 m. Locations of high LLJ frequency and duration across the state are seasonally varying with a mean duration of 3.5 hours. LLJ are most frequent in the topographically

15   complex northwest of the state in winter, and in the flatter northeast of the state in spring. Sensitivity of LLJ characteristics to the: i) LLJ definition and ii) vertical resolution at which the WRF output is sampled are examined. LLJ definitions commonly used in LLJ literature are considered in the first sensitivity analysis. These sensitivity analyses indicate that LLJ characteristics are highly variable with LLJ definition. Further, when the model output is down-sampled to lower vertical resolution, the maximum LLJ wind speed and mean height

20   decrease, but spatial distributions of regions of high frequency and duration are conserved.

1   Introduction

The term low-level jet (LLJ) is applied to any lower-tropospheric maximum of horizontal winds that exhibits confined vertical extent (Markowski and Richardson, 2011). LLJ are observed episodically in most regions of the world (Rife et al., 2010; Krishnamurthy et al., 2015). LLJ formation mechanisms and manifestations span a range

25   of scales from synoptic down to meso- and micro-scales (Blackadar, 1957; Chen and Kpaeyeh, 1993; Jiang et al., 2007). Mechanisms commonly invoked to describe the forcing mechanisms include diurnal variations in thermal forcing over sloping terrain (referred to as the Holton mechanism, (Holton, 1967)) and diurnal variations in boundary layer friction (referred to as Blackadar mechanism (Blackadar, 1957)). Both mechanisms invoke decoupling of the planetary boundary layer from the surface and indicate LLJ are most frequent under stable

30   conditions and hence at nighttime (Holton, 1967), and in areas with topographic and/or land cover variability (Parish, 1982). LLJ characteristics, such as frequency, intensity and duration also exhibit lower frequency variability that is expressed on seasonal and inter-annual timescales (Weaver et al., 2009; Liang et al., 2015).
In the continental US, the Southern Great Plains (SGP) LLJ is a persistent and prominent warm-season climate feature manifest at the synoptic scale; it extends over multiple degrees of longitude (i.e. having a width of hundreds

35   of kilometers) and is coherent over many degrees of latitude (i.e. the jet is oriented along a south-north axis parallel to the Rocky Mountains) (Weaver and Nigam, 2008; Rife et al., 2010). This jet is centered at heights below 850

hPa with a maximum (jet core) most commonly observed between 300-625 m height (Rife et al., 2010) and is associated with moisture flux and summertime precipitation (Higgins et al., 1997; Berg et al., 2015). Wind profiler observations at 250-m intervals from 500 m a.g.l. to 19 km from a network of 31 stations across the Great Plains

40   suggested the mean LLJ height was approximately 1000 m and the mean duration was 2 to 4 hours (Mitchell et al., 1995).

LLJ are observed across a range of spatial and temporal scales and in both onshore and coastal environments. Observational data derived using minisodars and wind profilers deployed at the ABLE facility in Kansas in the US Southern Great Plains indicated the presence of southerly (72%) and northerly (28%) LLJ and the wind

45   maxima typically occurred at 200-400 m a.g.l.. The southerly LLJ exhibited higher mean duration (~6.7 hours in the cold season and 6 hours in the warm season) than northerly jets (Song et al., 2005). LLJ at and below these altitudes have the potential to impact the wind speed, turbulence, and shear across typical wind turbine rotor planes (Gutierrez et al., 2014; Gutierrez et al., 2017; Nunalee and Basu, 2014; Wagner et al., 2019; Aird et al., 2020; Barthelmie et al., 2020). If LLJ speed maxima occur at or near the rotor plane, enhancements in turbulence and

50   shear have implications for turbine efficiency and blade loading and longevity (Kelley et al., 2005).

Despite the pertinence of LLJ characterization to wind resources and wind turbine operating conditions, a consistent and objective methodology for identifying and characterizing LLJ events is lacking. LLJ detection algorithms based on wind speed profiles employ:

    1) Combined criteria based on both the absolute wind speed maximum and the difference in wind speed
55   above and below the jet maxima (Bonner et al., 1968; Whiteman et al., 1997; Song et al., 2005).

    2) A minimum absolute threshold for the difference in wind speeds above and below the profile maximum (Andreas et al., 2000; Banta et al., 2002).

    3) A minimum threshold for wind speeds above and below the jet maxima defined as a percentage of the wind speed maximum.

60   4) A combination of (2) and (3), requiring both, or one of the two, thresholds to be met (Lampert et al., 2015; Baas et al., 2009).

Use of subjective and varying thresholds render inter-comparison of the frequency and/or intensity of LLJ across studies difficult. Adding to this ambiguity, some studies entirely lack a quantitative LLJ definition.

Variations in the resolution of observational data or model output used to identify LLJ also contribute to
65   ambiguity, inconsistencies in characterization, and/or a lack of generalizability (Kalverla et al., 2019; Whiteman et al., 1997; Bonner et al., 1968). For example, two analyses by Bonner et al. in 1968 and Whiteman et al. in 1997 of LLJ in the same region used similar criteria but differed in that the second study added a fourth LLJ criterion based on enhanced vertical resolution of rawinsonde data (Bonner et al. 1968; Whiteman et al. 1997). This led to detection of LLJ with stronger wind speeds and lower wind maxima than was found in the initial study.

70   Research presented herein uses output from a simulation conducted using the Weather Research and Forecasting (WRF) model to characterize LLJ occurrence and characteristics. The specific WRF configuration (e.g. selection of the planetary boundary layer (PBL) scheme) and horizontal and vertical resolution has a clear impact on simulated flow within the atmospheric boundary layer and LLJ properties, but in general WRF has been demonstrated to exhibit skill in simulating LLJ events and the near-surface wind climate (Storm et al., 2008;

75   Vanderwende et al., 2015; Squitieri et al., 2016; Smith et al., 2018; Schepanski et al., 2015; Pryor et al., 2020a). Here, we do not further explore these dependencies but rather analyse WRF output to (i) develop a LLJ

climatology over a region within the US with high wind turbine densities and topographic variability, (ii) quantify the dependence of the LLJ characteristics (frequency, intensity, duration) and rotor plane conditions to the precise criteria used to identify LLJ and (iii) investigate the impact of vertical resolution on LLJ characteristics using full resolution and down-sampled WRF output.

80

2 Methodology

2.1 WRF simulations

A high-resolution WRF (v3.8.1) simulation is conducted using a nested domain where the outer domain (D01) spans 150 by 150, 12×12 km grid cells and encompasses much of the US Midwest, while the inner domain (D02),

85 centered over Iowa, comprises 246 by 204 4×4 km grid cells (Pryor et al. 2020b) (Figure 1). A time step of 72 seconds is used for D01, while the time step in D02 is 24 seconds. 57 vertical sigma layers are employed and there are 25 levels below approximately 530 m a.g.l. Below 250 m a.g.l., the vertical spacing is approximately 15 m. Analyses presented here use once hourly model output for December 2007 to May 2008, and thus consider over 4300 profiles for each grid cell within a sub-domain (D03) comprising 147 by 100 grid cells that encompasses the

90 state of Iowa (Figure 1). Iowa was selected as the focus for this work due to the high density of wind turbines (nearly 11GW of installed capacity) (American Wind Energy Association, 2019) and observational research that has indicated a high frequency of extreme positive wind shear, which may be associated with LLJ (Walton et al., 2014). Key physics settings in the simulation presented here parallel those used in a similar study of the Orinoco LLJ over South America (Jiménez-Sanchéz et al., 2019); i.e. the Mellor-Yamada-Nakanishi-Niino 2.5 (Nakanishi

95 and Niino, 2006) PBL scheme is used, along with the MM5 surface layer scheme (Beljaars, 1995), and the Noah land surface model (Tewari et al., 2004). Note that in all analyses presented herein only wind speeds within the lowest 530 m of the atmosphere are considered. This implicitly limits the detection of LLJ to levels below that height.
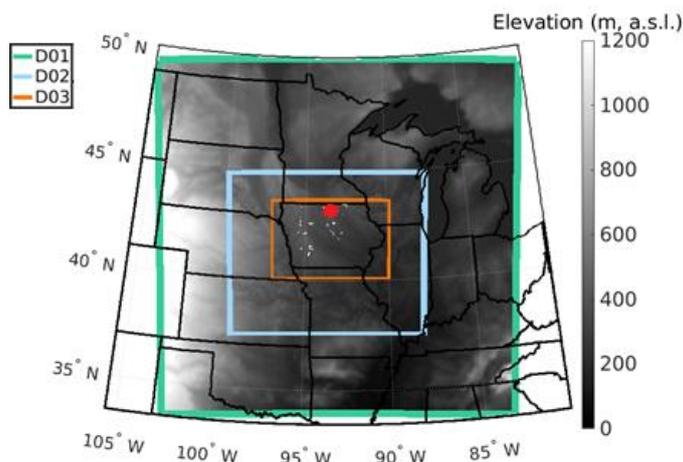
100 **Fig 1. Terrain elevation and domains used in the WRF simulation – D01, D02; and the region from which wind profiles are analyzed D03. White markers indicate wind turbine locations in 2014 (https://eerscmap.usgs.gov/uswtdb/). The red marker indicates the approximate location of the grid cell with highest LLJ frequency that is examined in Section 3.2.**

2.2 Climatology: LLJ identification and meteorological conditions

The climatology of LLJ characteristics over Iowa is developed using a detection algorithm that employs a *variable*

105 criterion of 20%, applied to WRF output for all grid cells. This detection algorithm means a LLJ is identified as present in a given profile if the wind speeds above and below the wind speed maximum have magnitudes that are at least 20% below the maximum (jet-core) wind speed. Thus, the threshold *varies* based on the maximum value in each wind speed profile. Cumulative density functions of atmospheric parameters conditionally sampled based on the presence or absence of a LLJ are used to describe the conditions associated with LLJ. The parameters

110 considered are: (a) Turbulent kinetic energy (TKE) derived by the PBL scheme. (b) Wind speed at a nominal hub-height of 100 m above ground level (a.g.l.). (c) The Richardson number across the nominal rotor plane (Ri_{Rotor}) specified as 50 – 150 m a.g.l. The Ri_{Rotor} is similar to the Bulk Richardson number (Stull, 1988) but describes the dynamical stability across the wind turbine rotor (Nunalee and Basu, 2014):

$$Ri_{Rotor} = \frac{2(Z_2 - Z_1)g}{\theta_{Z_2} + \theta_{Z_1}} \left[\frac{\theta_{Z_2} - \theta_{Z_1}}{(u_{Z_2} - u_{Z_1})^2 + (v_{Z_2} - v_{Z_1})^2} \right] \quad (1)$$

115 Where: U, u, v, and θ represent wind speed, wind speed components u and v, and virtual potential temperature, respectively, at height Z a.g.l. $Ri_{Rotor} \sim 0$ is indicative of near-neutral stability, $Ri_{Rotor} > 0.25$ indicates stable conditions, and $Ri_{Rotor} < 0$ indicates unstable conditions (Grachev et al., 2013).

(d) Shear across the nominal rotor plane:

$$Shear = \left(\frac{U_{Z_2} - U_{Z_1}}{Z_2 - Z_1} \right) \quad (2)$$

120 All variables except Ri_{Rotor} are computed at a disjunct hourly time step, while Ri_{Rotor} is computed using output disjunct at three hourly intervals.

Probability distributions for LLJ characteristics, including duration and the jet core height, are also examined. If a LLJ occurs in a grid cell, the cell is flagged for each hour of occurrence. To calculate duration, these flags are counted for each consecutive LLJ occurrence, representing the length of time in which output from a given grid

125 cell indicates the presence of a LLJ.

2.3 Sensitivity analyses

Following development of the climatology, two sensitivity analyses are performed (Table 1). The first sensitivity analysis (A) examines the impact of different detection algorithms on the resulting LLJ climatology. LLJ are detected and characterized using both; (i) *fixed* criteria i.e. a difference in wind speed above and below the wind

130 speed maximum quantified in absolute terms (Andreas et al., 2000; Banta et al., 2002). The five values used are 1:1:5 ms^{-1}. (ii) *variable* criteria i.e. a difference in wind speeds above and below the wind speed maximum expressed as a percentage of the wind speed maximum. The five thresholds used are 10:10:50%. Often, these two types of criteria are used in conjunction, requiring a fixed *or* variable threshold or a fixed *and* variable threshold to be met (Baas et al., 2009; Lampert et al., 2016). This study examines both definitions separately to define the

135 LLJ extracted under both types of thresholds. The criteria are described in five classes (groups) from the least strict (1 ms^{-1} fixed, 10% variable) to the strictest (5 ms^{-1} fixed, 50% variable) (Table 2).

Results from sensitivity analysis A are illustrated using the WRF grid cell with the highest LLJ frequency according to the climatology developed when a 20% variable criterion is selected (92.2784°W, 43.7467°N). Results are presented in terms of the mean LLJ profiles and the marginal probability of LLJ produced by each

140 criterion. From this, a relative frequency of disagreement is calculated between the two LLJ definitions in each criteria group, indicating how often definitions (for each level of strictness) identify different LLJ events. Across the entire domain, distributions of LLJ magnitude, duration, and jet core height are compared for each LLJ detection algorithm, and the domain-wide temporal LLJ frequency is compared for thresholds in criteria group 2 (2 ms^{-1} fixed, 20% variable).

145 **Table 1. Summary of the LLJ Sensitivity Studies A & B.**

Sensitivity study	Outline and Purpose	LLJ Identification Criteria	Output vertical sampling
A	Impact of different detection algorithms	5 Variable and 5 Fixed thresholds (Table 2)	Full resolution
B	Vertical resolution of wind speed output down-sampled	20% Reduction in wind speed above and below LLJ WS maximum	Full, half down-sample, quarter down-sample

Table 2. Criteria Groups for Sensitivity Study A. Also shown are the marginal probabilities of LLJ when each of the fixed and variable selection criteria are applied. Results are shown for hourly wind speed profiles from the single grid cell with highest LLJ frequency for a variable threshold of 20%.

Criteria Group	1	2	3	4	5
Fixed Criterion (ms^{-1})	1	2	3	4	5
Fixed: LLJ frequency	0.4110	0.2234	0.1116	0.0517	0.0198
Variable Criterion (% of maximum LLJ wind speed)	10	20	30	40	50
Variable: LLJ frequency	0.4087	0.2336	0.0970	0.0326	0.0132

150

Sensitivity analysis B is conducted to examine whether, and by how much, LLJ characteristics change with the vertical resolution at which the WRF output is sampled. Wind speed output is down-sampled to a half and a quarter of the simulation resolution to investigate effects of wind speed profile data resolution when all other factors are unchanged. Results of this analysis are presented in terms of the spatiotemporal mean LLJ wind speed

155 profiles, magnitude of the LLJ, duration, fraction of LLJ that impinge upon the rotor plane (defined as heights from 50-150 m a.g.l.) and the spatial patterns of LLJ frequency and duration.

3   Results

3.1   LLJ characterization using a variable threshold of 20%

A clear jet core is evident when comparing spatiotemporal mean LLJ and non-LLJ profiles normalized by each

160 profile's respective wind speed maximum (Figure 2). The spatiotemporal mean core wind speed computed using all hours from all grid cells of the LLJ is approximately 9.55 ms^{-1} and is centered at about 183 m a.g.l. Approximately 96% of LLJ exhibit jet core wind speeds of 3-25 ms^{-1} and are thus likely to be associated with normal wind turbine operation. Over the analysis period of six months there is evidence of a LLJ in one or more grid cells on nearly 98% of nights (between 8pm-6am local time) and nearly 65% of LLJ occur at night. Daytime

165 LLJ are more frequent in the winter months (December - February). Approximately 40% of winter LLJ occur during daytime hours as compared to 30% during spring (March – May).
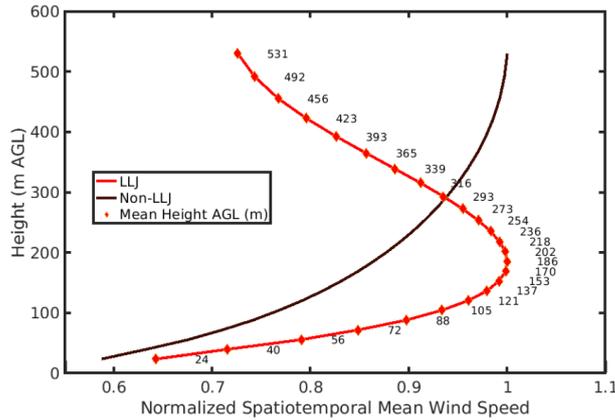
Fig 2. – Mean wind speed profiles during hour identified as exhibiting LLJ and those without (non-LLJ). These profiles are computed for all hourly profiles from all grid cells and each profile is normalized by the maximum wind speed after compositing. The LLJ detection algorithm uses a variable threshold of 20%. Both mean wind speed profiles are plotted against the temporally and spatially averaged mean height of each vertical level (◆).

Thirty-percent of LLJ are evident only in individual hours, but 4% have a duration of > 10 hours (Figure 3(a)). The modal value of LLJ height is between 100-150 m a.g.l. (the upper extent of the nominal rotor plane), and approximately 39% of LLJ have a wind speed maximum within the nominal rotor plane of 50-150 m (Figure 3(b)).
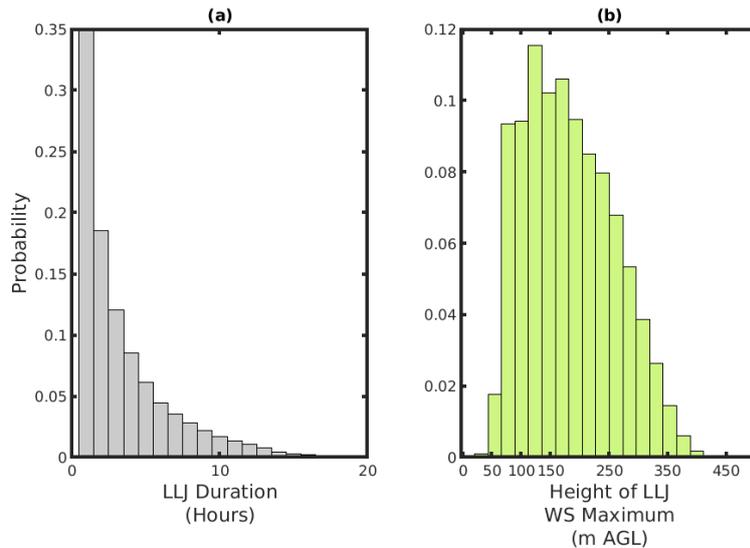
Fig 3. – Probability distributions from a domain-wide sample of all hourly realizations (n=4392) of vertical LLJ WS profiles for: (a) LLJ duration; (b) Height of the jet core. Note that LLJ with durations of over 20 hours were identified, but the distribution is truncated at 20 hours for legibility.

Consistent with expectations, LLJ are more prevalent during stable conditions as indicated by cumulative density functions of Ri_{Rotor}, conditionally sampled by the presence or absence of a LLJ (Figure 4(a)). Approximately 15% of LLJ occur during hours when Ri_{Rotor} <0.25, but the spatio-temporal median Ri_{Rotor} is 0.87 when the detection

algorithm indicates the presence of a LLJ. Conversely, 60% of non-LLJ profiles occur with Ri_{Rotor} <0.25, and the median non-LLJ Ri_{Rotor} is 0.15. Also consistent with a priori expectations, LLJ events are associated with

185 substantially lower TKE within the rotor plane. The median TKE within the rotor plane when LLJ are identified is 0.056 m^2s^2, while the non-LLJ median rotor plane TKE is 0.37 m^2s^2 (Figure 4(b)). Almost two-thirds (61%) of LLJ exhibit wind speed maxima above the rotor plane. Thus, a greater diversity (i.e. wider distribution) of wind shear conditions occur during LLJ (Figure 4(d)), and there is evidence that very near-surface (i.e. low altitude) LLJ can induce negative shear across the nominal rotor plane (Gutierrez et al. 2017). Wind speeds at the nominal

190 hub-height of 100 m a.g.l. are higher on average during non-LLJ conditions (Figure 4(c)), with a median of 9.24 ms^{-1} when compared to the LLJ median of 8.02 ms^{-1}. This is likely due to a complex combination of the following factors; (a) the LLJ selection criteria is more readily met at lower wind speeds (see below), (b) micro-scale to mesoscale features (i.e. locally forced LLJ) are less readily established under conditions with strong synoptic forcing that generates high geostrophic wind speeds (Mortarini et al., 2018) and (c) depending on the precise

195 height under consideration and the depth of the boundary layer, stable stratification may result in decreased vertical exchange of momentum (Barthelmie et al., 2013).
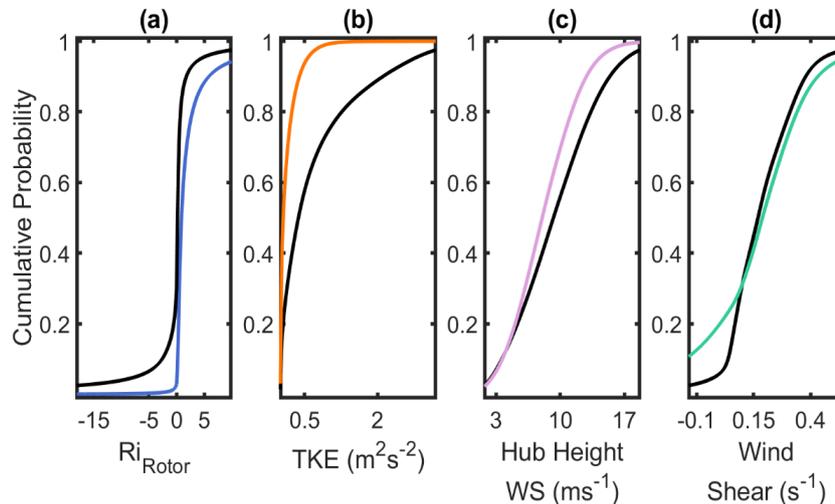
Fig 4. – Domain-wide spatiotemporal cumulative density functions for conditions during hours with LLJ (colored) and without (non-LLJ) (black): (a) Ri_{Rotor}; (b) mean TKE across the rotor plane; (c) hub height wind speed (wind speed at
200 **100 m a.g.l.); (d) –wind shear across the nominal rotor plane (50 to 150 m a.g.l.). For enhanced visibility, each subfigure is cropped at the 2.5th and 97.5th percentile values of non-LLJ parameters.**

The mean duration and frequency of LLJ exhibits a clear dependence on geographical location and season (Figure 5). On average, LLJ last slightly longer and occur more frequently in the winter months. The mean duration averaged over space and time is 3.6 hours in winter and 3.4 hours in spring. In spring, the northeast of Iowa

205 experiences the highest frequency of LLJ, with the detection algorithm using a 20% variable threshold detecting LLJ on up to 20% of hours. The mean LLJ duration in this season and region of Iowa approaches 4.5 hours. Conversely, the western part of the state is characterized by higher terrain elevation and larger terrain variability and exhibits a wintertime maximum of both LLJ duration and frequency (27% of hours) (Figure 5) consistent with formation of LLJ resulting from drainage-flow induced gravity waves (Prabha et al., 2011; Udina et al., 2013).

210   Mean wind vectors at a nominal wind turbine hub-height of ~ 100 m a.g.l. under LLJ and non-LLJ conditions suggest marked difference in both the mean wind direction in winter and spring and the mean wind directions (averaged in polar space) associated with LLJ and non-LLJ conditions (Figure 5(a) and (b)). The mean winter flow direction for both LLJ and non-LLJ is westerly, while easterly flow is more common during the spring months. Springtime LLJ are most frequently associated with northeasterly flow over the northeast of the state,

215   while winter LLJ are most frequently associated with southwesterly flow in the northwest of the state. Analyses of the seasonality and spatial variability of mean LLJ wind directions indicate that, during winter over the western portion of the state, LLJ are predominantly associated with southerly wind directions, while over eastern Iowa the LLJ are associated with more northerly flow (Figure 5a). Conversely, springtime LLJ over almost all of the state are dominated by easterly wind directions and are generally of substantially shorter duration over the western half
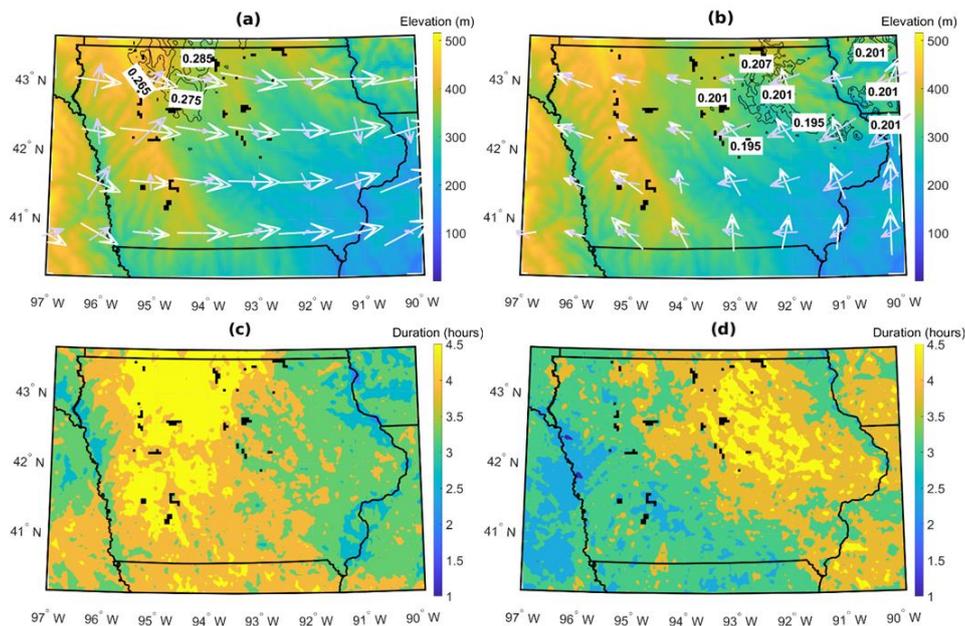
220   of Iowa (Figure 5).

Fig 5. – (a) – Dec-Feb. Regional elevation (m) with contours of regions of highest 10% of LLJ frequency (>.26). Average LLJ (—) and non-LLJ (white) wind vectors at nominal turbine hub height of 100 m; (b) – Mar-May. Regional elevation (m) with contours of regions of highest 10% of LLJ frequency (>.19). Average LLJ and non-LLJ wind vectors at
225   **nominal turbine hub height of 100 m; (c) – Dec-Feb. Regional mean LLJ duration; (d) – Mar-May. Regional mean LLJ duration. Black markers indicate wind turbine locations.**

This variation in LLJ intensity and duration by season and location may reflect differences in LLJ genesis mechanisms. The western portion of Iowa exhibits substantially more complex terrain and thus may be subject to stronger thermal (radiative) and dynamic forcing at the meso- and micro-scales. Consequently, this region may

230   be subject to density-driven slope and valley winds that may induce LLJ via the Holton mechanism, particularly during winter (Holton, 1967). The increase of LLJ frequency in the northeast during the spring is also associated with an increase in LLJ speed when compared to LLJ wind speeds for the region in winter and may have a greater forcing contribution from the Blackadar mechanism (Blackadar, 1957).

3.2 Sensitivity analyses: LLJ detection algorithm

235 Any LLJ climatology is naturally dependent on the detection algorithm applied. Thus, a sensitivity analysis is performed using differing LLJ detection thresholds (see Table 2). The impact of selecting different thresholds (five different fixed thresholds (1:1:5 ms⁻¹) and five different variable thresholds (10:10:50%)) is illustrated in Figure 6 for the WRF grid cell that exhibited the highest LLJ frequency using a 20% variable threshold (grid cell location indicated in Figure 1). As shown in Figure 6, the time-average mean wind speed profiles during hours

240 identified as exhibiting LLJ using these ten different selection criteria differ greatly. As the threshold used in the variable criterion increases, i.e. the difference between the LLJ core wind speed and the wind speeds above and below that level increases, the mean wind speed at the nominal wind turbine hub height and throughout the entire lowest 530 m of the model output decrease (Figure 6(a)). Conversely, as the fixed threshold for the difference in absolute wind speed of the jet core and above and below it increases from 1 to 5 ms⁻¹, wind speeds at the nominal

245 wind turbine hub height and throughout the entire lowest 530 m of the model output increase. These changes are non-linear and are most profound close to the mean height of the LLJ core (approx. 200 m a.g.l.). Alteration of the stringency of the threshold has a considerably more modest impact on the height at which the mean jet core is manifest (Figure 6).

Application of increasingly stringent criteria (higher thresholds) causes the overall frequency of LLJ to decrease

250 (Table 2). Interestingly, the absolute frequency of LLJ is consistent for criteria groups across the two methods (fixed and variable thresholds) (Table 2). However, the mean wind speed profiles differ markedly. For criteria group 2, which features the fixed and variable criteria used (independently and in conjunction) throughout literature (20% variable/2 ms⁻¹ fixed), the temporal mean wind speed maximum for variable is approximately 4ms⁻¹ lower than that of the fixed (Hallgren et al., 2020; Andreas et al., 2000; Kalverla et al., 2019; Duarte et al., 2012).
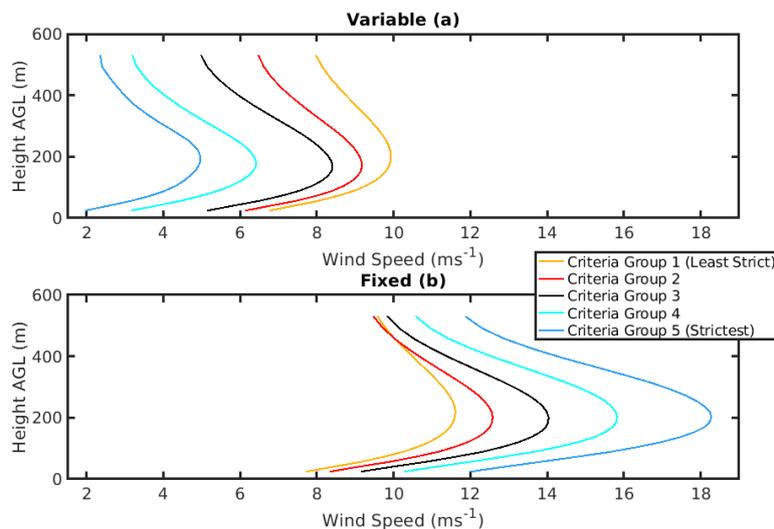
255

Fig 6. – Temporal mean LLJ wind speed profiles extracted by each criterion (variable – (a) and fixed – (b)), colored by criteria group (criterion utilized for climatology is shown in red as part of Criteria Group 2). Calculated from wind speed profiles sampled hourly from the single grid cell with highest LLJ frequency.

Despite similarity in the frequency with which LLJ are detected, the two criteria (even in the least strict criteria group of 1 ms^{-1} fixed, 10% variable) identify a substantial number of different, distinct LLJ events. For the least stringent criteria group, of the total number of times that a LLJ is identified between the two criteria (the intersection of identified LLJ), the criteria extract different LLJ events 20% of the time (i.e. a LLJ is identified by one type of criterion but not the other). Thus, the relative frequency of disagreement is 20%. This relative frequency of disagreement increases to nearly 40% for the second criteria group (2 ms^{-1} fixed, 20% variable) (Figure 7). The frequency with which LLJ are identified by variable criteria but not by fixed, and vice versa, is relatively equal for the first three criteria groups. However, as the thresholds increase (criteria groups 4 and 5), LLJ are more likely to be identified by fixed criteria than when the variable threshold is applied (Figure 7). When the most stringent thresholds are applied, the absolute frequency of LLJ decreases and over 90% of those cases are only detected by one of the two algorithms.
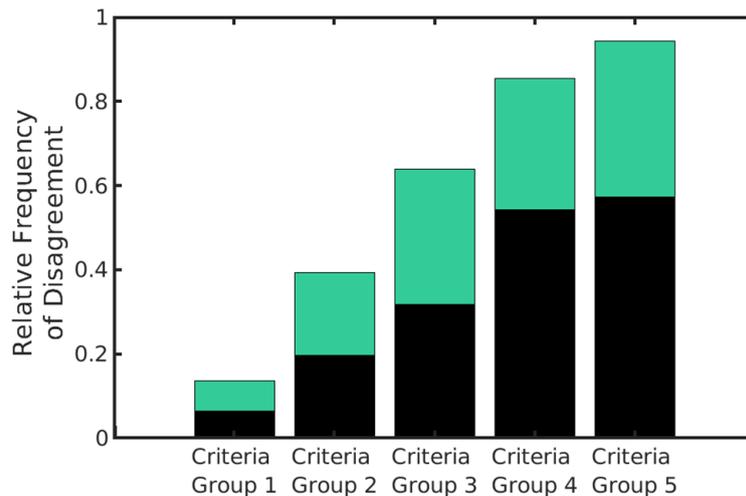
Fig 7. – Relative frequency of disagreement of LLJ identification between analyses using a fixed threshold and a variable threshold by criteria group. Relative frequencies shaded by the proportion of disagreements in which: a LLJ is identified by fixed criteria but not variable (black), a LLJ is identified by variable criteria but not fixed (green). Calculated from hourly output from single grid cell with highest LLJ frequency when the 20% variable criterion is applied (see Figure 1 for location).

Results of the sensitivity analyses applied to all grid cells within D03 and all hours during the six-month period are consistent with those from the individual grid cell with highest LLJ frequency. The median LLJ height is higher by approximately 20 m when the fixed wind speed thresholds are applied than in use of any of the variable thresholds (Figure 8(a)). Use of a higher variable threshold for LLJ detection (i.e. going from a deviation in wind speeds of 10% around the jet maximum to 50%) leads to a modest decline in the median height of the LLJ (Figure 8(a)) and a marked decline in LLJ duration from 6 hours to 2 hours (Figure 8(c)). Use of a stricter fixed threshold leads to an even smaller change in the median height of the LLJ maximum (Figure (8(b)). For all three properties, the LLJ cases become more self-similar (the dispersion of the distributions decreases) as increasingly selective criteria are applied (Figure 8). For all levels of strictness considered, variable criteria extract more cases that are identified as outliers (i.e. lie beyond 1.5 times the interquartile range from the 75th percentile) in terms of the LLJ duration than fixed criteria (Figure 8(c)). As in results for an individual grid cell shown in Figure 6, as the absolute

threshold for applied for LLJ detection increases, the LLJ maximum wind speed increases, whilst the converse is true for increasing the variable criteria threshold (Figure 8(b)).
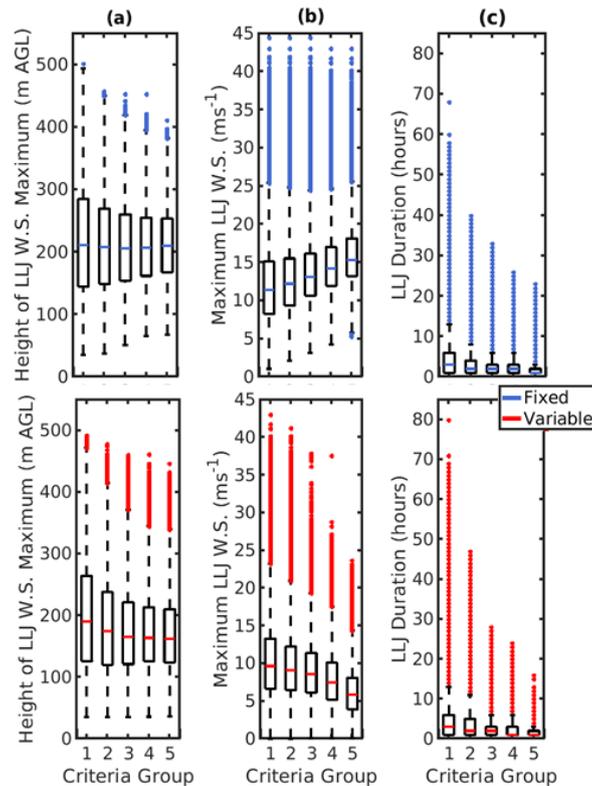
290 **Fig 8. – Box-whisker plots for definition-wise distributions of spatiotemporal LLJ characteristics (a) jet core height; (b) jet core speed; and (c) jet duration over the entire domain. Note: the whiskers on the boxplots extend from the 75th percentile to plus 1.5* times the inter-quartile range, and from the 25th percentile to 1.5* times the inter-quartile range. Points beyond those values are defined as outliers and plotted as individual points.**

For criteria group 2 (2 ms⁻¹ fixed, 20% variable), the spatial distribution of LLJ frequency differs markedly (Figure

295 9). As illustrated by Figure 7 using output for a single grid cell, it is evident that algorithms using the two different criteria flag different periods as indicative of the presence of LLJ. The tendency for variable criteria to extract lower wind speed LLJ and for fixed criteria to extract higher speed LLJ is potentially evident in frequency differences between groups across varying terrain; for the area of high elevation in the west of the state, fixed criteria extract a higher frequency of LLJ than variable criteria on the western side of the terrain elevation.

300 Conversely, on the eastern side, LLJ are extracted with higher frequency when a variable criterion is utilized. It is thus possible that variations in flow velocity over complex terrain contribute to the frequency differences in LLJ extracted by each criterion (Helbig et al., 2016). Areas with lower LLJ wind speed as defined in Figure 5 overlap with areas of higher LLJ frequency when a variable criterion is applied. The same is true for higher LLJ speeds when a fixed criterion is applied. The inference is that the two detection approaches, regardless of the

305 precise thresholds applied, may exhibit differing ability to identify the presence of a LLJ depending on the causal mechanism, which has implications for regional LLJ studies in complex terrain.
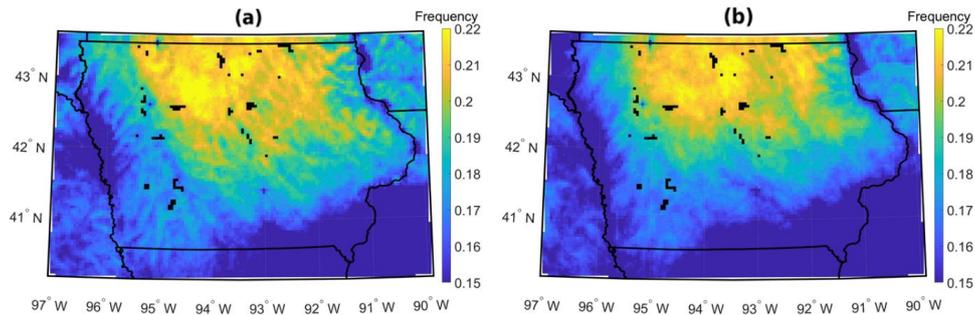
Fig 9. – Spatial distributions of LLJ frequency computed using a detection algorithm with a (a) 20% variable threshold, (b) 2 ms^{-1} fixed threshold.

310 **3.3   Sensitivity analyses: output resolution**

In this analysis, a LLJ detection algorithm using a variable threshold of 20% is applied to output from the WRF simulation using: the original vertical resolution, output sampled from every second level, and output sampled from every fourth vertical level (Table 3, Figure 10). The spatiotemporal mean LLJ core wind speed differs markedly according to the vertical resolution (Table 3). When the model output is sampled at one-quarter of the

315 simulation vertical resolution, the mean maximum (jet core) wind speed is 1 ms^{-1} lower than when the LLJ detection algorithm is applied to output at the model resolution (i.e. all 25 levels below 531 m a.g.l.) (Figure 10, Table 3). Output down-sampled to one quarter resolution also exhibits a substantially lower mean LLJ core height (156.43 m) than when the analysis is applied to output at full resolution (182.64 m). This reduction in the height of the wind speed maxima results in a higher percentage of LLJ cores falling within the nominal wind turbine

320 rotor plane of 50 – 150 m a.g.l.. The spatiotemporal mean duration and frequency of LLJ are also lower in the reduced resolution output (Table 3).
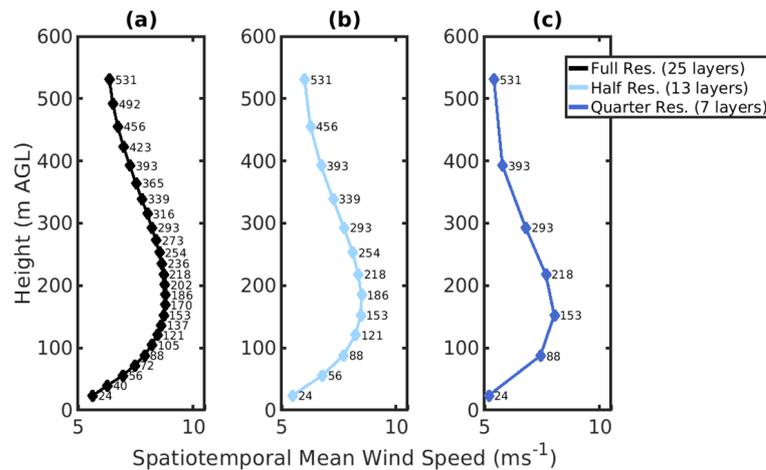
Fig 10. – Mean wind speed profiles for output at; (a) – full resolution (25 layers, no down-sampling); (b) – half resolution (13 layers, output down-sampled to every other layer); (c) – quarter resolution (7 layers, output down-sampled to every fourth layer).

325

Table 3. Spatially and temporally averaged LLJ properties as a function of model output vertical resolution.

	Mean Jet Core Wind Speed (ms⁻¹)	Mean Height of Jet Core (m a.g.l.)	Mean LLJ Duration (hours)	% LLJ with Jet Cores within the Rotor Plane	Spatiotemporal LLJ Frequency
Sensitivity Analysis B: Down-sampling of output					
Full Resolution: 25 Vertical levels	9.55	182.64	3.52	39.15	17.32%
13 Vertical levels	9.18	172.89	3.35	41.83	15.12%
7 Vertical levels	8.53	156.43	2.98	46.95	10.75%

Although the frequency of LLJ is sensitive to the model output resolution, if the mean LLJ frequency and duration in each WRF grid cell, as extracted from down-sampled and full resolution output, are normalized relative to their respective maximum values, the patterns of spatial variability are remarkably similar (Figure 11). Minimum and maximum differences between normalized frequency and duration range from approximately -0.2 to 0.2, respectively, indicating that spatial variability is conserved under reduced vertical resolution. Thus, the spatial patterns of LLJ frequency and duration are comparatively insensitive to the down-sampling of vertical resolution. That is, regions identified as having the highest frequency and temporal mean duration (the highest 5% of each quantity) of LLJ are similar when the LLJ detection algorithm is applied to output at the original vertical resolution and one-quarter vertical resolution (Figure 11(a)). However, there is more divergence in spatial variation of LLJ duration than frequency (Figure 11(b)). This potentially indicates that inter-study comparisons of regions of high LLJ frequency (and less so duration) may be possible, even under reduced vertical resolution of observational data and/or model output.
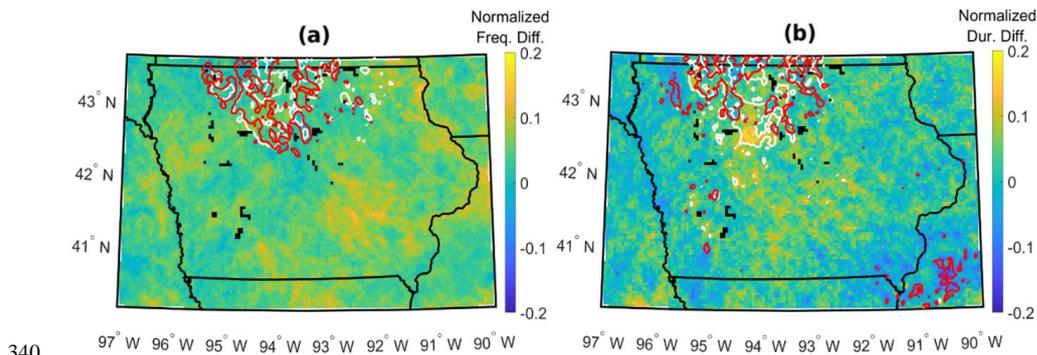
Fig 11. –Mean spatial results for Dec. 2007 – May 2008, inclusive. Maps colored by difference in (a) normalized LLJ frequency and (b) normalized LLJ duration for output at full resolution and down-sampled to 7 layers. Contours represent regions of highest 5% of (a) LLJ frequency and (b) LLJ duration for output at full resolution (white) and down-sampled to 7 layers (red).

4   Conclusions

High resolution WRF simulations over the state of Iowa for December 2007-May 2008 are analyzed to generate a climatology of LLJ over the state and to assess the implications for wind energy resources and operating conditions. Properties considered are: maximum wind speed, height of the wind speed maximum, frequency, duration, and flow direction. Using a detection algorithm in which the wind speed above and below the LLJ must decrease by at least 20% of the jet core wind speed, approximately 95% of LLJ have wind speed maxima between 3 and 25 ms⁻¹ and the mean, modal and median height of the LLJ core are approximately 183, 125, and 174 m,

respectively. LLJ are found to be associated with low TKE across the rotor plane (50-150 m a.g.l.), to occur most frequently under stable conditions, and to cause comparatively high positive and occasionally negative wind shear across the rotor plane. LLJ are most common in the north of the state. Locations of highest regional LLJ frequency

355 and duration are found to exhibit seasonal variability, likely due to changes in flow direction and the interaction between regional and locally forced flows.

Assessments of the sensitivity to the precise detection algorithm applied and output resolution are also performed. The first sensitivity analysis is conducted at full model output resolution and is designed to determine the sensitivity of LLJ characteristics to changes in LLJ definition. Two common types of criteria for LLJ definition

360 are studied, labeled as *variable* and *fixed* criteria. Five criteria in each definition are considered (5 variable, 5 fixed) and are grouped by criteria strictness, ranging from 1 ms^{-1} (fixed) to 10% (variable) for the least strict criteria group (criteria group 1), and 5 ms^{-1} (fixed) to 50% (variable) for the strictest (criteria group 5). Sensitivity to LLJ definition is first illustrated for a single grid cell in the domain that exhibits the highest value of temporal LLJ frequency. Using different LLJ definitions is shown to identify not just different frequencies of LLJ but also

365 different LLJ events. When considering all LLJ identified by the least strict criteria group, the definitions are shown to extract different LLJ for nearly 20% of the time. For the second criteria group that features LLJ definitions used in previous LLJ literature (2 ms^{-1} fixed and 20% variable), the two definitions extract different LLJ (i.e. one definition flags a LLJ while the other does not) 40% of the time. Using output from all grid cells within the state of Iowa, it is shown that all LLJ characteristics are sensitive to changes in LLJ definition.

370 A second sensitivity study is conducted to determine the sensitivity of LLJ characteristics to changes in vertical resolution of the wind speed output. WRF output is down-sampled to one-half and one-quarter of the simulation resolution prior to application of the LLJ detection algorithm. All LLJ characteristics considered are found to be sensitive to reductions in wind speed profile vertical resolution but, as expected, characteristics calculated at ½ vertical resolution exhibit small percent differences from values at full vertical resolution when compared to those

375 calculated at ¼ resolution, indicating that sensitivity to vertical resolution of wind speed data is non-linear. While LLJ frequency and duration are sensitive numerically to output resolution, there is good agreement for the spatial variability of those properties. These findings indicate that, while numerical values among LLJ studies may differ due to changes in wind speed profile vertical resolution, regions of high LLJ frequency may be correctly identified.

Data availability.

380 All of the hourly WRF output is available upon request from the authors via the DoE HPPS system.

Author contributions.

JAA, RJB and SCP jointly designed the analysis framework. JAA, RJB and SCP developed methods. JAA designed the sensitivity study analysis. JAA developed the figures, and drafted the initial paper with input from RJB and SCP. TJS performed the WRF simulations and SCP obtained the computing resources. SCP and RJB

385 also contributed to the writing of the final paper.

Competing interests.

The authors declare that they have no conflict of interest.

Acknowledgements.

The authors gratefully acknowledge support by the U.S. Department of Energy (DoE) (DE-SC0016438 and DE-
390   SC0016605), the National Science Foundation (NSF) Graduate Research Fellowship Program (DGE-1650441),
and computing resources from the NSF (ACI-1541215 and TG-ATM170024) and DoE (DE-AC02-05CH11231).

References

Aird, J. A., Barthelmie, R. J., Shepherd, T. J., and Pryor, S. C.: WRF-Simulated Springtime Low-Level Jets Over
Iowa: Implications for Wind Energy, J. Phys. Conf. Ser., 1618(6), 062020, doi:10.1088/1742-
395   6596/1618/6/062020, 2020.

American Wind Energy Association: US Wind Industry Fourth Quarter 2019 Market Report., 2019.

Andreas, E. L., Claffey, K. J., and Makshtas, A. P.: Low-level atmospheric jets and inversions over the western
Weddell Sea, Boundary-Layer Meteorol., 97(3), 459–486, doi:10.1023/A:1002793831076, 2000.

Baas, P., Bosveld, F. C., Klein Baltink, H., and Holtslag, A. A. M.: A climatology of nocturnal low-level jets at
400   Cabauw. J. Appl. Meteorol. Climatol, 48(8), 1627-1642, doi:10.1175/2009JAMC1965.1, 2009.

Banta, R. M., Newsom, R. K., Lundquist, J. K., Pichugina, Y. L., Coulter, R. L., and Mahrt, L.: Nocturnal Low-
Level Jet Characteristics Over Kansas During Cases-99, Boundary-Layer Meteorol., 105(2), 221-252,
doi:10.1023/A:1019992330866, 2002.

Barthelmie, R. J., Hansen, K. S., and Pryor, S. C.: Meteorological controls on wind turbine wakes, Proc. IEEE,
405   101(4), 1010-1019, doi:10.1109/JPROC.2012.2204029, 2013.

Barthelmie, R. J., Shepherd, T. J., Aird, J. A., and Pryor, S. C.: Power and Wind Shear Implications of Large
Wind Turbine Scenarios in the US Central Plains, Energies, 13(16), 4269, doi:10.3390/en13164269, 2020.

Beljaars, A.: The parametrization of surface fluxes in large-scale models under free convection, Q. J. R. Meteorol.
Soc., 121(522), 255-270, doi:10.1002/qj.49712152203, 1995.

410   Berg L. K., Riihimaki L. D., Qian, Y., Yan, H., and Huang, M.: The low-level jet over the Southern Great Plains
determined from observations and reanalyses and its impact on moisture transport, J. Climate, 28(17), 6682–6706.
doi: 10.1175/JCLI-D-14-00719.1, 2015.

Blackadar: Boundary Layer Wind Maxima and Their Significance for the Growth of Nocturnal Inversions, Bull.
Amer. Meteor., 38(5), 283-290, doi:10.1175/1520-0477-38.5.283, 1957.

415   Bonner, W. D.: Climatology of the Low Level Jet, Mon. Weather Rev., 96(12), 833–850, doi:10.1175/1520-
0493(1968)096<0833:cotllj>2.0.co;2, 1968.

Chen, T. C. and Kpaeyeh, J. A.: The synoptic-scale environment associated with the low-level jet of the Great
Plains, Mon. Weather Rev., 121(2), 416–420, doi:10.1175/1520-0493(1993)121<0416:tsseaw>2.0.co;2, 1993.

Duarte, H. F., Leclerc, M. Y., and Zhang, G.: Assessing the shear-sheltering theory applied to low-level jets in
420   the nocturnal stable boundary layer, Theor. Appl. Climatol., 110(3), 359-371, doi:10.1007/s00704-012-0621-2,
2012.

Grachev, A. A., Andreas, E. L., Fairall, C. W., Guest, P. S., and Persson, P. O. G.: The critical Richardson number and limits of applicability of local similarity theory in the stable boundary layer, Boundary-Layer Meteorol., 147(1), 51-82, doi:10.1007/s10546-012-9771-0, 2012.

425   Gutierrez, W., Araya, G., Basu, S., Ruiz-Columbie, A., and Castillo, L.: Toward Understanding Low Level Jet Climatology over West Texas and its Impact on Wind Energy, J. Phys. Conf. Ser., 524(1), 012008, doi:10.1088/1742-6596/524/1/012008, 2014.

Gutierrez, W., Ruiz-Columbie, A., Tutkun, M., and Castillo, L.: Impacts of the low-level jet's negative wind shear on the wind turbine, Wind Energy Sci., 2(2), 533-545, doi:10.5194/wes-2-533-2017, 2017.

430   Hallgren, C., Arnqvist, J., Ivanell, S., Körnich, H., Vakkari, V., and Sahlée, E.: Looking for an offshore low-level jet champion among recent reanalyses: a tight race over the Baltic Sea, Energies, 13(14), 3670, doi:10.3390/en13143670, 2020.

Helbig, N., Mott, R., Van Herwijnen, A., Winstral, A., and Jonas, T.: Parameterizing surface wind speed over complex topography, J. Geophys. Res. Atmos., 122(2), 651-667, doi:10.1002/2016JD025593, 2016.

435   Higgins, R. W., Yao, Y., Yarosh, E. S., Janowiak, J. E., and Mo, K. C.: Influence of the Great Plains low-level jet on summertime precipitation and moisture transport over the central United States, J. Climate, 10(3), 481-507, doi: 10.1175/1520-0442(1997)010<0481:IOTGPL>2.0.CO;2, 1997.

Holton, J. R.: The diurnal boundary layer wind oscillation above sloping terrain, Tellus, 19(2), 200–205, doi:10.3402/tellusa.v19i2.9766, 1967.

440   Jiang, X., Lau, N. C., Held, I. M,. and Ploshay, J. J.: Mechanisms of the Great Plains low-level jet as simulated in an AGCM, J. Atmos. Sci., 64(2), 532–547, doi:10.1175/JAS3847.1, 2007.

Jiménez-Sánchez, G., Markowski, P. M., Jewtoukoff, V., Young, G. S., and Stensrud, D. J.: The Orinoco Low-Level Jet: An Investigation of Its Characteristics and Evolution Using the WRF Model, J. Geophys. Res. Atmos., 124(20), 10696-10711, doi:10.1029/2019JD030934, 2019.

445   Kalverla, P. C., Duncan, J. B., Steeneveld, G. J., and Holtslag, A. A. M.: Low-level jets over the north sea based on ERA5 and observations: Together they do better, Wind Energy Sci., 4(2), 193–209, doi:10.5194/wes-4-193-2019, 2019.

Kelley, N. D., Jonkman, B. J., Scott, G. N., Bialasiewicz, J. T., and Redmond, L. S.: Impact of coherent turbulence on wind turbine aeroelastic response and its simulation, No. NREL/CP-500-38074, National Renewable Energy

450   Lab (NREL), Golden, CO (United States), 2005.

Klein, P. M., Hu, X. M., Shapiro, A., and Xue, M.: Linkages between boundary-layer structure and the development of nocturnal low-level jets in Central Oklahoma, Boundary-Layer Meteorol., 158(3), 383-408, doi:10.1007/s10546-015-0097-6, 2015.

Krishnamurthy, L., Vecchi, G. A., Msadek, R., Wittenberg, A., Delworth, T. L., and Zeng, F.: The seasonality of

455   the great plains low-level Jet and ENSO relationship, J. Clim., 28(11), 4525–4544, doi:10.1175/JCLI-D-14-00590.1, 2015.

Lampert, A., Bernalte Jimenez, B., Gross, G., Wulff, D., and Kenull, T.: One-year observations of the wind distribution and low-level jet occurrence at Braunschweig, North German Plain, Wind Energy, 19(10), 1807–1817, doi:10.1002/we.1951, 2016.

460   Liang, Y. C., Yu, J. Y., Lo, M. H., and Wang, C.: The changing influence of El Niño on the Great Plains low-level jet, Atmos. Sci. Lett., 16(4), 512–517, doi:10.1002/asl.590, 2015.

Markowski, P. and Richardson, Y.: Mesoscale Meteorology in Midlatitudes, Wiley-Blackwell, Chichester, UK, 2011.

Mitchell, M. J., Arritt, R. W., and Labas, K.: A climatology of the warm season Great Plains low-level jet using
465   wind profiler observations, Weather Forecast., 10(3), 576–591, doi:10.1175/1520-0434(1995)010<0576:ACOTWS>2.0.CO;2, 1995.

Mortarini, L., Cava, D., Giostra, U., Acevedo, O., Nogueira Martins, L., Soares de Oliveira, P., and Anfossi, D.: Observations of submeso motions and intermittent turbulent mixing across a low level jet with a 132-m tower, Q. J. R. Meteorol. Soc., 144(710), 172-183, doi: 10.1002/qj.3192, 2018.

470   Nakanishi, M. and Niino, H.: An improved Mellor–Yamada level-3 model: Its numerical stability and application to a regional prediction of advection fog, Boundary-Layer Meteorol., 119(2), 397-407, doi:10.1007/s10546-005-9030-8, 2006.

Nunalee, C. G. and Basu, S.: Mesoscale modeling of coastal low-level jets: implications for offshore wind resource estimation, Wind Energy, 17(8), 1199–1216, doi:10.1002/we.1628, 2014.

475   Parish, T. R.: Barrier winds along the Sierra Nevada mountains, J. Appl. Meteor., 21(7), 925-930, doi:10.1175/1520-0450(1982)021<0925:BWATSN>2.0.CO;2, 1982.

Prabha, T. V., Goswami, B. N., Murthy, B. S., and Kulkarni, J. R.: Nocturnal low-level jet and "atmospheric streams" over the rain shadow region of indian western ghats, Q. J. R. Meteorol. Soc., 137(658), 1273–1287, doi:10.1002/qj.818, 2011.

480   Pryor, S. C., Shepherd, T. J., Bukovsky, M., and Barthelmie, R. J.: Assessing the stability of wind resource and operating conditions, J. Phys. Conf. Ser., 1452(1), doi:10.1088/1742-6596/1452/1/012084, 2020a.

Pryor, S. C., Shepherd, T. J., Volker, P. J. H., Hahmann, A. N., and Barthelmie, R. J.: "Wind Theft" from onshore wind turbine arrays: Sensitivity to wind farm parameterization and resolution, J. Appl. Meteorol. Climatol., 59(1), 153–174, doi:10.1175/JAMC-D-19-0235.1, 2020b.

485   Rife, D. L., Pinto, J. O., Monaghan, A. J., Davis, C. A., and Hannan, J. R.: Global distribution and characteristics of diurnally varying low-level jets, J. Clim., 23(19), 5041–5064, doi:10.1175/2010JCLI3514.1, 2010.

Schepanski, K., Knippertz, P., Fiedler, S., Timouk, F., and Demarty, J.: The sensitivity of nocturnal low-level jets and near-surface winds over the Sahel to model resolution, initial conditions and boundary-layer set-up, Q. J. R. Meteorol. Soc., 141(689), 1442-1456, doi:10.1002/qj.2453, 2015.

490   Smith, E. N., Gibbs, J. A., Fedorovich, E., and Klein, P. M.: WRF Model study of the Great Plains low-level jet: Effects of grid spacing and boundary layer parameterization, J. Appl. Meteorol., 57(10), 2375-2397, doi:10.1175/JAMC-D-17-0361.1, 2018.

Song, J., Liao, K., Coulter, R. L., and Lesht, B. M.: Climatology of the low-level jet at the southern Great Plains atmospheric boundary layer experiments site, J. Appl. Meteorol., 44(10), 1593-1606, doi:10.1175/JAM2294.1,
495   2005.

Squitieri, B. J. and Gallus, W. A.: WRF forecasts of Great Plains nocturnal low-level jet-driven MCSs. Part II: Differences between strongly and weakly forced low-level jet environments, Weather Forecast., 31(5), 1491-1510, doi:10.1175/WAF-D-15-0150.1, 2016.

Storm, B., Dudhia, J., Basu, S., Swift, A., and Giammanco, I.: Evaluation of the weather research and forecasting
500   model on forecasting low-level jets: Implications for wind energy, Wind Energy, 12(1), 81-90, doi:10.1002/we.288, 2008.

Stull, R. B.: An Introduction to Boundary Layer Meteorology, Kluwer, Dordrecht, The Netherlands, 1988.

Tewari, M., Chen, F., Wang, W., Dudhia, J., LeMone, M., Mitchell, K., Ek, M., Gayno, G., Wegiel, J., and Cuenca, R.: Implementation and verification of the unified NOAH land surface modelin the WRF model, 20th Conference

505   on Weather Analysis and Forecasting/16th Conference on Numerical Weather Prediction, 1115(6), 10-15, 2004.

Udina, M., Soler, M. R., Viana, S., and Yagüe, C.: Model simulation of gravity waves triggered by a density current, Q. J. R. Meteorol. Soc., 139(672), 701-714, doi:10.1002/qj.2004, 2012.

Vanderwende, B. J., Lundquist, J. K., Rhodes, M. E., Takle, E. S., and Irvin, S. L.: Observing and Simulating the Summertime Low-Level Jet in Central Iowa, Mon. Weather Rev., 143(6), 2319–2336, doi:10.1175/MWR-D-14-

510   00325.1, 2015.

Vosper, S. B., Ross, A. N., Renfrew, I. A., Sheridan, P., Elvidge, A. D. and Grubišić, V.: Current challenges in orographic flow dynamics: Turbulent exchange due to low-level gravity-wave processes, Atmosphere (Basel)., 9(9), 1–18, doi:10.3390/atmos9090361, 2018.

Wagner, D., Steinfeld, G., Witha, B., Wurps, H., and Reuder, J.: Low level jets over the southern North Sea,

515   Meteorol. Z., 28(5), 389–415, doi:10.1127/metz/2019/0948, 2019.

Walton, R. A., Takle, E. S., and Gallus, W. A.: Characteristics of 50-200m winds and temperatures derived from an Iowa tall-tower network, J. Appl. Meteorol. Climatol., 53(10), 2387–2393, doi: 10.1175/JAMC-D-13-0340.1, 2014.

Weaver, S. J., and Nigam, S.: Variability of the Great Plains low-level jet: Large-scale circulation context and

520   hydroclimate impacts, J. Climate, 21(7), 1532-1551, doi:10.1175/2007JCLI1586.1, 2008.

Weaver, S. J., Schubert, S., and Wang, H.: Warm season variations in the low-level circulation and precipitation over the central United States in observations, AMIP simulations, and idealized SST experiments, J. Climate, 22(20), 5401-5420, doi: 10.1175/2009JCLI2984.1, 2009.

Whiteman, C. D., Bian, X., and Zhong, S.: Low-Level Jet Climatology from Enhanced Rawinsonde Observations

525   at a Site in the Southern Great Plains, J. Appl. Meteorol., 36(10), 1363–1376, doi:10.1175/1520-0450(1997)036<1363:LLJCFE>2.0.CO;2, 1997.